Dispersion Corrections to Forces at Planar Surfaces

Linnea Lundberg[1] and Olle Edholm[1,*]
[1] *Theoretical Biological Physics, Department of Theoretical Physics, Royal Institute of Technology (KTH), AlbaNova University Center, SE-106 91 Stockholm, Sweden*

[*]Corresponding author. Electronic address: `oed@kth.se`.

Abstract

It is known that a cutoff on the van der Waals interactions in molecular dynamics simulations of systems containing a surface (gas/liquid for instance) may cause substantial changes in the densities of the different parts of the system. In order to make the density independent of the cutoff, we have calculated forces from continuum integrations and added them to the forces calculated in a molecular dynamics program. These corrections compensate for the lack of long range interactions and exert a pressure on the system that may be several hundred bars. We show here that inclusion of such corrections makes the density profile independent of the cutoff. This makes it possible to calculate a surface tension that is independent of the cutoff.

Introduction

It has been noticed (1) that usage of a cutoff on the attractive part of Lennard-Jones interaction may have a much bigger effect on surface properties like surface tension than on bulk properties of the systems. In the bulk, isotropic dispersion corrections are simple and work very well. Anisotropic dispersion corrections can be calculated at a surface assuming that the variation of the number densities of different types of atoms as a function of the distance from the surface are known (2–6). Although this may require numerical calculations, analytical approximations work quite well and result in corrections to the surface tension that, to a good approximation, decrease proportional to the cutoff radius to the power of minus 2. Alternatively an Ewald method may of course be used for the attractive r^{-6} interactions as well as for the electrostatics (7). The method to calculated dispersion corrections to the surface tension after performing a simulation works very well for systems were the main part of the cohesion comes from other force than the van der Waals forces. For some systems, like Lennard-Jones fluids, we note that the structure of the surface is strongly affected by the cutoff. The usage of a short cutoff will lead to a lower density of the liquid and sometimes to a fairly dense gas outside the liquid. This is due to that the shorter cutoff corresponds to an effective weakening of the van der Waals forces that keep the system liquid. In these cases a straight-forward application of anisotropic dispersion corrections does not yield the correct surface tension. We have therefore calculated and implemented a correction that is applied to the force in the molecular dynamics simulations that mends this problem and results in a density profile that is independent of the cutoff. It is here shown how this is done and implemented in a molecular dynamics software. When anisotropic corrections to the surface tension is applied in this case, we get excellent agreement between simulations using different cutoffs and those based an Ewald treatment of the dispersion interactions.

Theory

For the attractive part of the van der Waals interactions we have the potential and force between two atoms i and j

$$U_{ij}(r_{ij}) = -\frac{C_{ij}^6}{r_{ij}^6} \text{ giving the force } \mathbf{F}_{ij} = -\nabla U_{ij} = \frac{6C_{ij}^6}{r_{ij}^8}\mathbf{r}_{ij}. \qquad (1)$$

When there are different atoms in the system, the parameters, C_{ij}^6, may either be given as a table or calculated as a geometrical or arithmetic average of parameters C_i^6 and C_j^6 for the different atom types. Whatever way this is done does not matter for the present treatment. The long-range tail correction from distances outside a cutoff, r_c to the force on atom i can then be written as a sum over all other atoms, j

$$\mathbf{F}_i = 6 \sum_j \frac{C_{ij}^6}{r_{ij}^8} \mathbf{r}_{ij} \approx 6 \iiint_{r_{ij} \geq r_c} C_{ij}^6 \rho_j^V(\mathbf{r}_j) \frac{\mathbf{r}_{ij}}{r_{ij}^8} \, \mathrm{d}^3 r_j. \tag{2}$$

The sum has now been replaced by an integral over a continuum number density $\rho_j^V(\mathbf{r}_j)$. We may define a dispersion density as

$$\rho_i^{\mathrm{disp}}(\mathbf{r}_j) = \sum_j C_{ij}^6 \rho_j^V(\mathbf{r}_j), \tag{3}$$

which will have dimension energy times length to the power 3 (note that this notation is different from our previous work (1)). This makes it possible to write the tail correction to the forces as the integral

$$\mathbf{F}_i^{\mathrm{tail}} = 6 \iiint_{r_{ij} \geq r_c} \rho_i^{\mathrm{disp}}(\mathbf{r}_j) \frac{\mathbf{r}_{ij}}{r_{ij}^8} \, \mathrm{d}^3 r_j. \tag{4}$$

From now on the superscripts 'tail' and 'disp' will be suppressed to simplify the notation. We specialize further to the case with planar geometry with

$$\rho_i(\mathbf{r}_j) = \rho_i(z_j). \tag{5}$$

and introduce cylindrical coordinates in the integral. For symmetry reasons, the force will then just have a z-component, which may we written as the double integral

$$F_{iz}(z_i) = 12\pi \iint_{(z-z_i)^2 + r^2 \geq r_c^2} \mathrm{d}z \, \mathrm{d}r \frac{r \rho_i(z)(z - z_i)}{[(z - z_i)^2 + r^2]^4}. \tag{6}$$

The force can be numerically evaluated for different shapes of the dispersion density, $\rho_i(z)$. For the special case of a sharp interface (centered at $z = 0$), the integral can be analytically solved. With

$$\rho_i(z) = \rho_i^0 - \frac{\Delta\rho_i^0}{2} + \Delta\rho_i H(z) \tag{7}$$

($H(z)$ being a Heaviside function), we get zero contribution from the constant term, while the other term gives a solvable integral. The solution can be written (suppressing the index i) as

$$F_z(z) = \frac{\pi}{2}\frac{\Delta\rho}{z^4} \text{ for } |z| \geq r_c \tag{8}$$

and

$$F_z(z) = \frac{3\pi}{2}\frac{\Delta\rho}{r_c^4}\left(1 - \frac{2}{3}(z/r_c)^2\right) \text{ for } |z| \leq r_c. \tag{9}$$

This may be simplified further by introducing the dimensionless force $f(u) = r_c^4 F_z/\Delta\rho$ and dimensionless length $u = z/r_c$

$$f(u) = \frac{3\pi}{2u^4} \text{ for } |u| \geq 1 \tag{10}$$

and

$$f(u) = \frac{3\pi}{2}(1 - \frac{2}{3}u^2) \text{ for } |u| \leq 1. \tag{11}$$

A tanh-shaped interface

We do, however, directly turn to a slightly more general case. A more realistic density profile, that can be justified theoretically in some cases (and also often is quite well reproduced by simulations), is the tanh-profile (see e.g. Safran (8))

$$\rho(z) = \rho^0 + \frac{\Delta\rho}{2}\tanh(z/d) \tag{12}$$

where ρ^0 is the average dispersion density and $\Delta\rho$ the difference between the two regions, while the parameter d describes the extension of the interface region. In the limit when d goes to zero, we are back at the sharp Heaviside function profile. The tail correction for the force is now

$$F_{iz}(z_i) = 6\pi\Delta\rho \iint_{(z-z_i)^2+r^2\geq r_c^2} \mathrm{d}z\,\mathrm{d}r \frac{r\tanh(z/d)(z-z_i)}{[(z-z_i)^2+r^2]^4}. \tag{13}$$

By variable substitutions this integral may be written as

$$F_{iz}(z_i) = 6\pi\Delta\rho \int_{r_c}^{\infty}\int_0^{\pi} \mathrm{d}\varphi\,\mathrm{d}R\ R^{-5}\sin\varphi\cos\varphi\tanh\left[(R\cos\varphi + z_i)/d\right]. \tag{14}$$

Using the dimensionless variables the force can now be written as a function of two variables

$$f(u = z_i/r_c, d/r_c) = 6\pi \int_1^\infty \int_0^\pi \mathrm{d}\varphi\, \mathrm{d}R\ R^{-5} \sin\varphi \cos\varphi \tanh\left[\frac{r_c}{d}(R\cos\varphi + u)\right] = \tag{15}$$

$$= 3\pi \int_0^1 \int_0^\pi \mathrm{d}\varphi\, \mathrm{d}x\ x^3 \sin(2\varphi) \tanh\left[\frac{r_c}{d}(\cos\varphi/x + u)\right]. \tag{16}$$

This integral is easily evaluated numerically. In Fig 1, the dimensionless force is plotted versus the distance from the interface ($u = z/r_c$) for a couple of values for d/r_c.

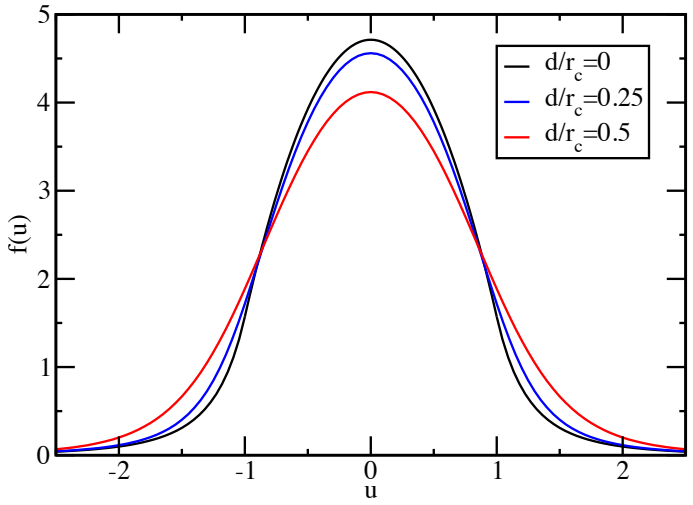

Figure 1: The dimensionless long range dispersion force perpendicular to a flat surface versus the dimensionless distance from the interface. The results are shown for a sharp surface and for a couple of d-values from a tanh-surface.

The correction to the surface tension derived in (1), which is also based on the tanh-density profile, is

$$\gamma^{\mathrm{tail}} = \frac{3\pi(\Delta\rho')^2}{8r_c^2}\left[1 - \frac{\pi^2}{6}\left(\frac{d'}{r_c}\right)^2 + 3.53\left(\frac{d'}{r_c}\right)^4 + ...\right], \tag{17}$$

where $\Delta\rho'$ is the difference in dispersion density, $\rho'(\mathbf{r}) = \sum_c \sqrt{C_6^c}\rho_V^c(\mathbf{r})$, which for a cyclohexane surface is 2.307×10^{-20} J and d' is the extension

of the surface in the $\rho'(\mathbf{r})$ profile, which for this system is 0.5 nm. In the general multi-component case, we assume here that the C_6 parameters can be obtained as geometrical averages for different atom types.

Simulations

The simulations in this work were performed using a modified version of the GROMACS 4.6.7 (9–11) code. Here, the software was altered and external forces were added close to the surfaces during run-time. The system was started as a cyclohexane/vacuum surface, although a small number of molecules evaporated during the simulation and we eventually got a dilute gas outside the fluid. Cyclohexane was modeled as a Lennard-Jones solvent with parameters developed in (1) shown in table 1. The system sizes and setup are presented in table 2. The run-time for the simulations were 10 ns. The system was started up as a bulk NpT-simulation where the periodic box after equilibration was increased by a factor 2 in the z-direction. Thereafter the simulation was continued in the NVT-ensemble. The temperature in the simulations was 300 K and was maintained using the V-rescale (12) thermostat.

Parameter	Cyclohexane (1)
σ [nm]	0.56180
ϵ [kJ/mol]	4.08650
C_6 [J/mol nm^6]	513.90
C_{12} [mJ/mol nm^{12}]	16.157

Table 1: The Lennard-Jones parameters for cyclohexane.

System(1/2)	V [nm^3]	2L [nm]	A [nm^2]	V_1/ V_2 [%]	N
CH/vacuum	1966.27	20.0	98.31	50/50	5331

Table 2: System parameters. The volume (V) and length in the normal direction (2L) of the system including the vacuum/gas part. The area (A) is a square in the lateral (xy) plane. V_n is the volume in percent of the cyclohexane and vacuum parts respectively in the initial configuration. N is the number of cyclohexane molecules.

In figure 2 the forces that compensate for the absence of long-range forces are shown for a 10 nm cyclohexane slab in physical units (pN) calculated from figure 1 using the parameter d=0.5 nm. We note that the force is anti-symmetric around the center of the slab and acts to compress the fluid. We also note that since it decays inversely proportional to the fourth power of the cutoff length, it soon becomes negligible when the cutoff is increased. For a 1 nm cutoff this force corresponds to a pressure of about 300 bar.

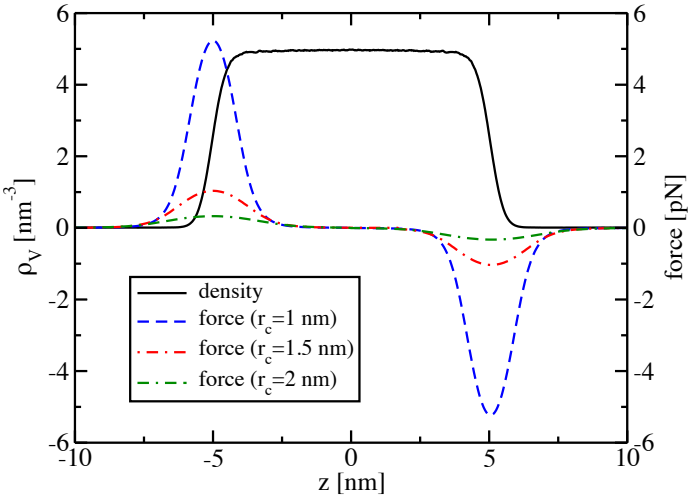

Figure 2: The density profile for a 10 nm slab of cyclohexane together with the added forces that compensate for the lack of long-range interactions.

Results and Discussion

The result of adding corrections to the forces can be seen in figure 3, where the solid purple line is the density-profile of the cyclohexane/vacuum-system at 1 nm cutoff without any corrections added. This profile compared to the profile where no cutoff is added (LJ-PME) shows a significant difference in density; the bulk density is substantially smaller when using a cutoff of 1 nm and there are more molecules present in the 'vacuum'-part of the system. The reason for this difference in density is that the interactions holding the system together are weaker due to the short cutoff used for the van der Waals interactions. When adding corrections to the forces we see that the density-profile, when using the 1 nm cutoff, is almost identical to the density-profile with no cutoff (LJ-PME).

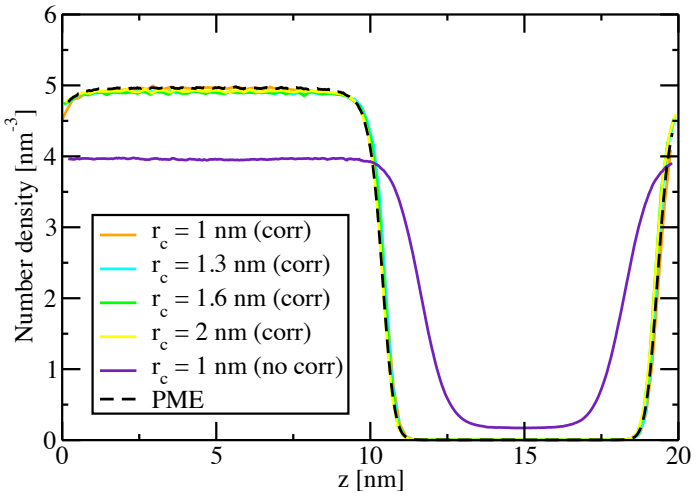

Figure 3: The density profile of a cyclohexane/vacuum-system with added corrections to the forces. The solid purple line without any corrections is for comparison.

When adding the corrections not only to the forces, but also to the surface tension (equation 17), we get the result seen in figure 4. This shows that when first adding the corrections to the forces, it is possible to add the corrections to the surface tension to produce a surface tension that is constant and independent of cutoff. In the figure this is shown by comparing the by comparing the blue circles, which represents the surface tension calculated in the simulation when corrections to the forces are added, to the dashed

blue line which represents the theoretically calculated surface tension. The purple triangles have additional corrections to the surface tension added and we see that the resulting surface tension is almost constant.

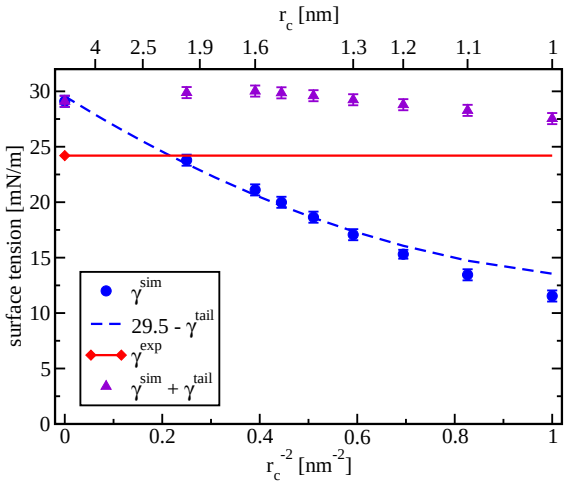

Figure 4: The surface tension of a cyclohexane surface with corrections added to the forces and to the surface tension. The experimental value is 24.2 mn/m at 300 K (13).

Conclusions

In our previous work (1) we noted that a short cutoff has a significant impact on the density-profile of a cyclohexane surface. This is because short cutoffs on the the van der Waals interactions weaken the interactions keeping the cyclohexane fluid together, resulting in a lowering of the density. In (1) we added corrections to the surface tension, but for this system, the corrections could not compensate entirely for the neglected interactions which is why additional corrections were needed. When adding corrections to the forces, the densities obtained with and without cutoff are negligible and the corrections to the surface tension developed in (1) can be added, which results in a surface tension that does not depend on the cutoff.

References

1. Lundberg, L., and O. Edholm, 2016. Dispersion Corrections to the Surface Tension at Planar Surfaces. Submitted.

2. Kirkwood, J., and F. P. Buff, 1949. The Statistical Mechanical Theory of Surface Tension. *The Journal of Chemical Physics* 17:338–343.

3. Chapela, G. A., G. Saville, S. M. Thompson, and J. S. Rowlinson, 1977. Computer simulation of a gas-liquid surface. Part 1. *J. Chem. Soc., Faraday Trans. 2* 73:1133–1144.

4. Blokhuis, E., D. Bedeaux, C. Holcomb, and J. Zollweg, 1995. Tail corrections to the surface tension of a Lennard-Jones liquid-vapour interface. *Molecular Physics* 85:665–669.

5. Neyt, J.-C., A. Wender, V. Lachet, A. Ghoufi, and P. Malfreyt, 2014. Quantitative Predictions of the Interfacial Tensions of Liquid–Liquid Interfaces through Atomistic and Coarse Grained Models. *Journal of Chemical Theory and Computation* 10:1887–1899.

6. Nijmeijer, M. J. P., A. F. Bakker, C. Bruin, and J. H. Sikkenk, 1988. A molecular dynamics simulation of the Lennard-Jones liquid–vapor interface. *The Journal of Chemical Physics* 89:3789–3792.

7. Wennberg, C. L., T. Murtola, B. Hess, and E. Lindahl, 2013. Lennard-Jones Lattice Summation in Bilayer Simulations Has Critical Effects on Surface Tension and Lipid Properties. *Journal of Chemical Theory and Computation* 9:3527–3537.

8. Safran, S. A., 1994. Statistical Thermodynamics of Surfaces, Interfaces, and Membranes. Addison-Wesley, Boulder, CO, USA.

9. Lindahl, E., B. Hess, and D. van der Spoel, 2001. GROMACS 3.0: a package for molecular simulation and trajectory analysis. *Journal of Molecular Modeling* 7:306–317.

10. van der Spoel, D., E. Lindahl, B. Hess, G. Groenhof, A. E. Mark, and H. J. C. Berendsen, 2005. GROMACS: Fast, flexible, and free. *Journal of Computational Chemistry* 26:1701–1718.

11. Pronk, S., S. Páll, R. Schulz, P. Larsson, P. Bjelkmar, R. Apostolov, M. R. Shirts, J. C. Smith, P. M. Kasson, D. van der Spoel, B. Hess, and

E. Lindahl, 2013. GROMACS 4.5: a high-throughput and highly parallel open source molecular simulation toolkit. *Bioinformatics* 29:845–854.

12. Bussi, G., D. Donadio, and M. Parrinello, 2007. Canonical sampling through velocity rescaling. *The Journal of Chemical Physics* 126:014101.

13. Lam, V. T., and G. C. Benson, 1970. Surface tensions of binary liquid systems. I. Mixtures of nonelectrolytes. *Canadian Journal of Chemistry* 48:3773–3781.